Master's Thesis
석사 학위논문

Sensor fusion for enhanced location tracking in virtual reality microsurgical environments

JOHN DAVID PRIETO PRADA(존프라다)

Department of
Robotics Engineering

DGIST

2018

Sensor fusion for enhanced location tracking in virtual reality microsurgical environments

Advisor: Professor Cheol Song
Co-advisor: Professor Jihwan Choi

by

JOHN DAVID PRIETO PRADA
Department of Robotics Engineering
DGIST

A thesis submitted to the faculty of DGIST in partial fulfillment of the requirements for the degree of Master of Science in the Department of Energy Science & Engineering. The study was conducted in accordance with Code of Research Ethics[1]

03. 07. 2018

Approved by

Professor Cheol Song (signature)
(Advisor)

Professor Jihwan Choi (signature)
(Co-Advisor)

[1] Declaration of Ethical Conduct in Research**:** I, as a graduate student of DGIST, hereby declare that I have not committed any acts that may damage the credibility of my research. These include, but are not limited to: falsification, thesis written by someone else, distortion of research findings or plagiarism. I affirm that my thesis contains honest conclusions based on my own careful research under the guidance of my thesis advisor.

Sensor fusion for enhanced location tracking in virtual reality microsurgical environments

JOHN DAVID PRIETO PRADA

Accepted in partial fulfillment of the requirements for the degree of Master of Science.

03. 07. 2018

Head of Committee _____ (signature)
Prof. Cheol Song

Committee Member _____ (signature)
Prof. Jihwan Choi

Committee Member _____ (signature)
Prof. Taiwoo Park

MS/RT
201623014

John David Prieto Prada. Sensor fusion for enhanced location tracking in virtual reality microsurgical environment. 2018. 38p. Advisors Prof. Cheol Song, Co-Advisors Prof. Jihwan Choi.

ABSTRACT

For a delicate micromanipulation, subjects need to perform tasks while effectively minimizing their hand tremor. Recently, there is growing interest in creating virtual reality (VR) microsurgery systems to enable enhanced visual feedback for precise manipulation tasks as well as a training environment. For an accurate micro-location, it is needed the use of various sensors (sensor fusion) which encompasses different ways of combining data through algorithms in order to refine information quality or derive more information about it. To enable precise location tracking of surgical tools (e.g., forceps), we propose a VR microsurgical environment featuring a sensor fusion algorithm for location tracking system with an additional inertial measurement unit (IMU). The system reconstructs an image of surgical instruments (i.e., forceps) and 2D figures with a zoomed view of them, to help surgeons have a more precise sense in visual feedback. We hypothesize that merging two different sensors and matching them in a Kalman filter algorithm, the micro-localization will be more accurately. We develop and test two ways, that is, (1) location tracking without Kalman filter, and (2) location tracking with Kalman filter activated. A performance evaluation of location tracking in terms of error has been conducted in real and virtual experiments. The result shows that the condition with sensor fusion activated achieves more precise location tracking than without Kalman filter condition.

Keywords: Virtual reality, Sensor fusion, Kalman filter, Micro-surgery, Healthcare.

Contents

List of Figures

List of Tables

1. Introduction

1.1 Study Background

The precision and safe manipulation of the medical device is essential, particularly in surgical applications. The manipulation performance is limited by the physiological capacity of a human. For example, physiological hand tremor has a frequency of 6-12 Hz with an amplitude of 100 μm [1], and it hinders accurate and successful microsurgery operation. To address this challenge, various assistive microsurgical systems have been developed, such as Micron [2] and SMART [3].

Figure 1. SMART forceps tool

1.2 Previous Studies

1.2.1 Virtual reality applications

Virtual reality (VR) technology has been highlighted recently in many industrial and biomedical fields. It has previously been applied to robotics micromanipulation [4], military skills in soldiers [5], phobia treatment, post-traumatic stress disorder [6], motor skill training on athletes [7], and surgical skill improvement [8]. The potential of VR has specifically been explored for the purpose of training subjects such as tele-operators for micro-robotic cell injection [9], for assembly procedures for microelectromechanical system prototypes that allow a supervisor to guide the task remotely [10], and in simulators that teach a subject how to perform an industrial assembly task through realistic scenarios and virtual environments [11]. These applications enable the subject to gain valuable experience in accurate tasks. Subjects learn or improve skills and techniques without causing harm to themselves or damaging any real tools, and communication skills can also be taught through a range of scenarios with virtual subjects [12].

1.2.2 The importance of virtual reality

Eyesight, or vision, is one of the main sources of information that plays an important role in VR [13, 14]. VR can both provide real-time virtual images and simulate virtual challenges by adjusting difficulty levels represented in the virtual world [15, 16]. It is known that visual inputs and spatial models are able to improve subjects' manipulation performance according to the level of awareness between the subjects and VR objects [17]. Simulation software, such as DIVE (Distributed Interactive Virtual Environment) [18], provides a virtual experimental environment for the development of multi-user virtual reality application. It has editable and distributed platforms where the user awareness can be experienced during the simulation. Also,

VR environments are enjoyable and lead the subjects to have a self-control of the experiment along the task [19]. In addition, by using the self-controlled long-term learning, VR can assist the subjects to overcome their phobias [20]. We envision that subjects could gain better control over their hand tremor if they train themselves in a VR environment, according to the research that manipulation skills can be learned through VR [21]. Implementation of a vision-based control on handheld manipulator has already been demonstrated [22]. The performance of handheld manipulator, Micron, was evaluated by tracking virtual fixtures, however, it is only available for tracking the instrument. Moreover, haptics-based VR systems have been presented for surgical training simulator [23]. These simulators allow the subjects to be well-trained in the virtual surgical tasks like bone dissection, making them comprehensive of it by giving an immediate force feedback to them. Nevertheless, the simulators just present the surgical procedures to the trainees without any visual modifications, aiming for adjustment in the procedure itself.

1.2.3 Visual stimuli in virtual reality to reduce hand tremor

A VR-based system that reconstructs an image of a handheld gripper with emphasized hand tremor was proposed. Provided with a modified visual feedback, in which subjects will develop better self-awareness of the tremor and thus control it more effectively. Two methods for visual modification were demonstrated to emphasize the hand tremor in VR: (1) tremor amplification and (2) object size magnification, in comparison to a control condition without any modifications. A human-subject study with twelve trials was conducted, using four healthy participants who performed a task based on minimizing hand tremor while holding the gripper in a certain direction. The results showed that the two proposed visual modification methods achieved reduced hand tremor compared with the control condition [24]. The proposed approach in this study highlights self-awareness as a key component. In figure 2, the user

watches these in the virtual world, and two elements - the green gripper (green mesh), and the virtual gripper (same as the real world) are modeled. Figure 3 shows the experiment with the gripper holding task has exemplified that the increase in self-awareness gained using VR technology could help users to reduce the angular element of hand tremor by 42% (from 3.242 to 1.868) and 29% (from 3.242 to 2.304), on average, using tremor amplification (M1) and object magnification (M2), respectively, without use of active tremor compensation technology such as SMART [1] and Micron [2].

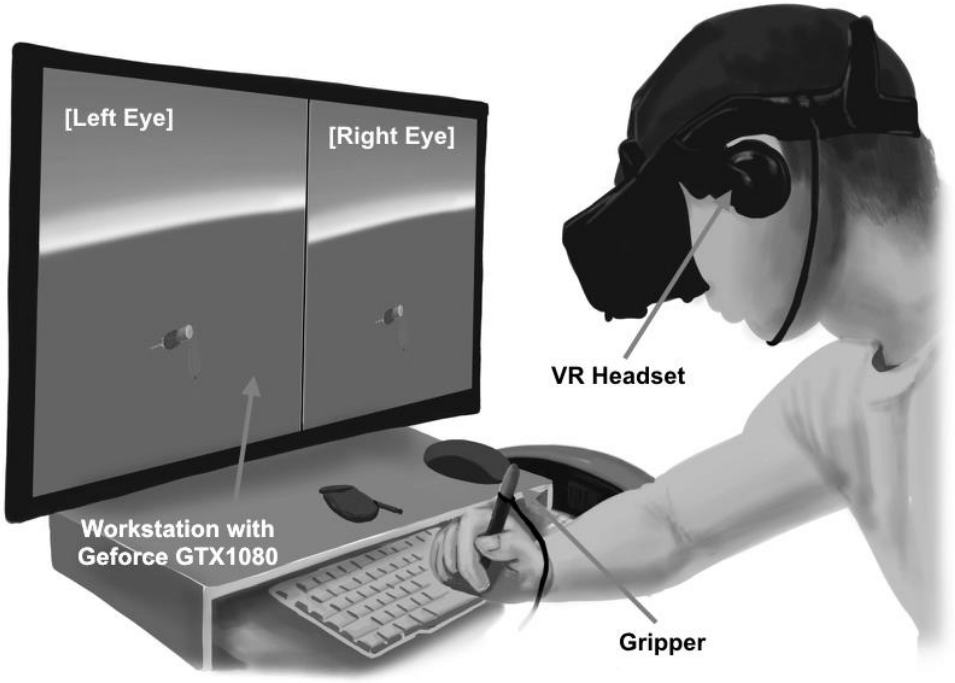

Figure 2. Visual stimuli in VR

It is worthwhile to note that the tremor amplification (M1) approach exaggerates users' hand tremor, which may show the user's handheld object (e.g., gripper or forceps) with a different relative position from that in real physical space, despite its greater potential for hand tremor reduction over the object magnification approach (M2). Considering the effectiveness of this method in micromanipulation tasks in practice, two ways to harness the tremor amplification approach were proposed. First, tremor amplification can be used for pre-task training sessions,

which can help users to understand their hand tremor pattern prior to actual micromanipulation tasks. The users will then be able to adjust their posture or pay particular attention to regulating their hand tremor. Second, the amplified tremor may be presented as assistive information, not directly applied to the object image in a VR environment.

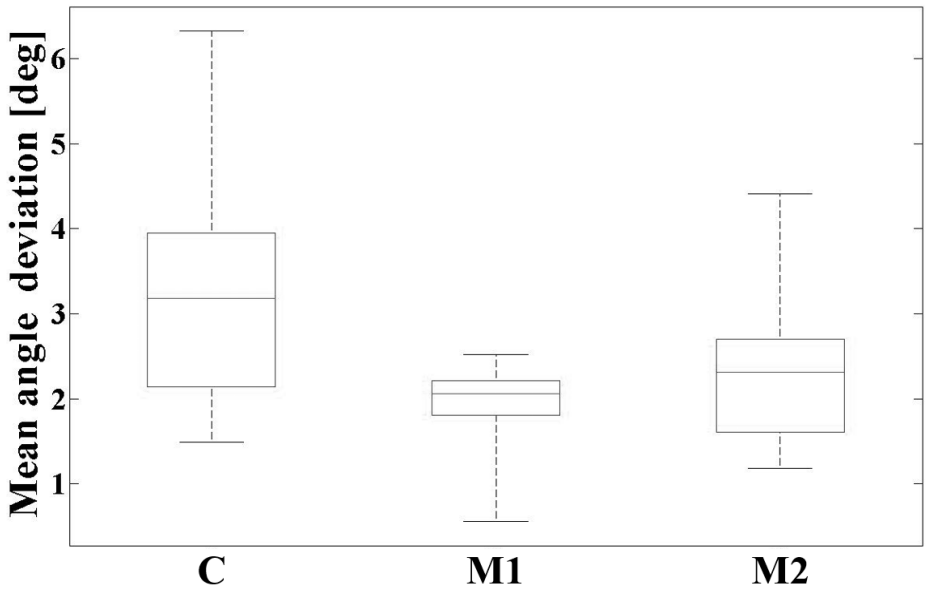

Figure 3. Visual stimuli in VR results

1.3 Study Purpose

In this study, we present a virtual reality (VR)-based micro-localization training system. By employing motion sensor-enabled forceps and a regular VR controller, the system shows a virtual image of forceps in a virtual space, with two alternative ways to precisely track position information. We applied a sensor fusion technique (Kalman filter) between a VR controller and an additional inertial measurement unit (IMU) and compared it with a Kalman filter deactivated condition. Experiments results indicate that a Kalman filter algorithm can give more precision in the micro-localization in VR environment.

2. Sensor Fusion

The sensor fusion is a combination of sensors data or data coming from different sources, thus, that the resulting information has less uncertainty than if these sources were used individually. In this case, the term uncertainty reduction means more accurate, more complete, or more reliable, or may refer to the result of an emerging view, such as stereoscopic vision (calculation of depth information by combining two-dimensional images of two cameras with slightly different image viewpoints). The data sources for a fusion process should not come from identical sensors. One can distinguish direct fusion, indirect fusion, and fusion of the outputs of the former two. Direct Fusion is the fusion of sensor data from a range of heterogeneous or homogeneous sensors, soft sensors, and historical values of sensor data, while indirect fusion uses information sources such as a priori knowledge of the environment and human input. Sensor fusion is also known as (multi-sensor) data fusion and is a subset of information fusion.

2.1 Sensor Fusion Algorithms

Sensor fusion covers a number of methods and algorithms:

- Bayesian networks
- Dempster-Shafer
- Convolutional neural network
- Kalman filter

2.1.1 Bayesian network

A Bayesian network, Bayes network, belief network, Bayesian model (Bayes) or probabilistic model in an acyclic graph directed in a probabilistic graph model (a type of static

model) that represents a set of random variables and their conditional dependencies through a directed acyclic graph. In Figure 4, it is indicated the uncertain quantities A, B, C, and the directed arrows between them to represent relationships. A Bayesian network encodes a joint probability distribution over all the nodes in the graph. In this case, our Bayes' net encodes the joint probability distribution, P (A, B, C, D). For example, the Bayesian network can succeed in approaching the problem of sequential estimation of the state of a dynamic system by using a sequence of noisy measurement. Formally, Bayesian networks are acyclic directed graphs whose nodes represent random variables in the Bayes sense: the same observable variables, latent variables, unknown parameters or hypotheses. The edges represent conditional dependencies; the nodes that are not connected represent variables which are conditionally independent of the others Each node has a probability function that takes as input a particular set of values of the parent variables of the node and returns the probability of the variable represented by the node. For example, if parents are m Boolean variables then the probability function can be represented by a table of 2 entries, an entry for each of the 2 possible combinations of the principles by the way or false. Ideas can be applied to non-directed, and possibly cyclic, graphs; as are the so-called Markov networks.

There are efficient algorithms that carry out inference and learning in Bayesian Networks. Bayesian networks that model sequences of variables are called dynamic Bayesian networks. The generalizations of Bayesian networks that can represent and solve decision problems under uncertainty are called influence diagrams.

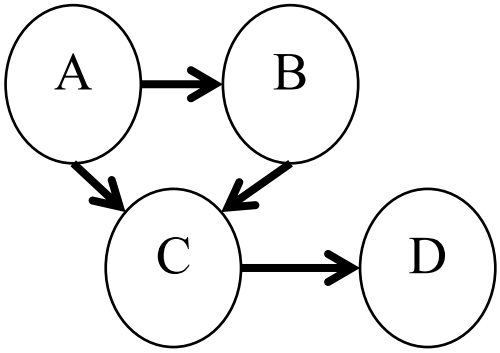

Figure 4. A Bayesian network

In order to analyze and make inferences about a dynamic system usually two models are required:

- System or dynamic model: it describes the evolution of the state along the time.

$$x_k = f_{k-1}(x_{k-1}, n_{k-1}) \tag{2}$$

Where $x_k \in n_x$ and n_{k-1} are the system noise.

- Measurement model: it relates the noisy measurements with to the state.

$$z_k = h_k(x_k, w_k) \tag{3}$$

Where $x_k \in n_z$ and w_k is the measurement noise.

Assuming that the models to be described in a probabilistic form, the Bayesian approach provides a rigorous general framework for dynamic state estimation. The main idea of the Bayesian approach to dynamic state estimation is to construct the posterior probability density function (pdf) of the state x_k based on all available information, including the sequence of received measurements $Z_k = z_{1:k}$

In other words, the optimal estimate of the state can be obtained from the posterior pdf.

Recursive filtering provides an estimate sequentially every time that a new measurement is available. This solution is well suited for the tracking problem where state estimate (position and velocity) is usually required for each time interval.

2.1.2 Dempster-Shafer

The Dempster-Shafer theory is a mathematical theory based on the functions of belief and the credible (reasoning) used to combine separate information (evidence) to calculate the probability of an event. The theory was developed by Arthur P. Dempster and Glenn Shafer.

In a narrow sense, the term Dempster–Shafer theory refers to the original conception of the theory by Dempster and Shafer. However, it is more common to use the term in the wider sense of the same general approach, as adapted to specific kinds of situations. In particular, many authors have proposed different rules for combining evidence, often with a view to handling conflicts in evidence better.

Formally, D-S theory is based on a finite set of p elements $S = \{S_1, S_2, \dots, S_p\}$, called a frame of discernment. A mass value is a function $m = 2^S$ ranging the subset between [0, 1] such that m (0) = 0 (0 – the empty set) and:

$$\sum_{S \in 2^S} m(S) = 1 \tag{4}$$

(2^S – the power set of S). Any proper subset s of the frame of discernment S, for which $m(S)$ is non-zero, it is called the focal element and represents the exact belief in the proposition depicted by S. The notion of a proposition here, being the collection of the hypotheses represented by the elements in a focal element.

The set of mass values associated with a single piece of evidence is called a body of evidence (BOE), often denoted $m(-)$. The mass value $m(S)$ assigned to the frame of discernment S

is considered the amount of ignorance within the BOE, and it represents the level of exact belief that cannot be discerned to any proper subsets of S.

D-S theory also provides a method to combine the BOE from different pieces of evidence, using Dempster's rule of combination. This rule assumes these pieces of evidence are independent:

$$(m_1 \oplus m_2)(x) = \begin{cases} 0, & x = \emptyset \\ \dfrac{\sum_{S_1 \cap S_2 = x} m_1(S_1) m_2(S_2)}{1 - \sum_{S_1 \cap S_2 = \emptyset} m_1(S_1) m_2(S_2)}, & x \neq \emptyset \end{cases} \quad (5)$$

Where S_1 and S_2 are focal elements from the BOEs, m1 (S) and m2 (S), respectively.

2.1.3 Convolutional neural networks

Convolutional Neural Networks (**ConvNets** or **CNNs**) are a category of Neural Networks that have proven very effective in areas such as image recognition and classification. ConvNets have been successful in identifying faces, objects and traffic signs apart from powering vision in robots and self-driving cars. A CNN consists of an input and an output layer, as well as multiple hidden layers. The hidden layers of a CNN typically consist of convolutional layers, pooling layers, fully connected layers and normalization layers. Description of the process as a convolution in neural networks is by convention. Mathematically it is a cross-correlation rather than a convolution. This only has significance for the indices in the matrix, and thus which weights are placed at which index.

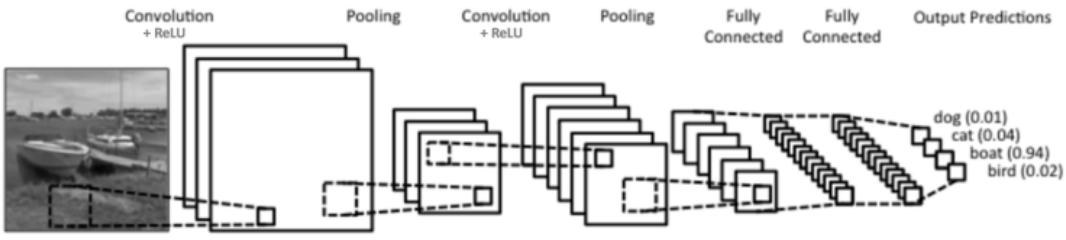

Figure 5. A simple ConvNet

As evident from the figure 5, on receiving a boat image as input, the network correctly assigns the highest probability for boat (0.94) among all four categories. The sum of all probabilities in the output layer should be one (explained later in this post).

There are four main operations in the ConvNet shown in Figure 5 above:

1. Convolution
2. Non Linearity (ReLU)
3. Pooling or Sub Sampling
4. Classification (Fully Connected Layer)

2.2 Sensor Fusion Methods

Generally, the task of a sensor is to provide information about a process variable in the environment by taking measurements. Since these measurements can be noisy and are - at least in digital systems - taken at discrete points in time, it is necessary to fuse multiple measurements to reconstruct the parameter of interest.

2.2.1 Smoothing

In figure 6 (a), the change of a process entity shall be reconstructed after a series of measurements have been performed. For each instance of interest, several measurements from previous, actual, and following instants are used in order to estimate the value of the process variable.

While the measurements have to be recorded in real time, the smoothing algorithm can be performed offline.

2.2.2 Filtering

In figure 6 (b), the actual state of a process entity shall be estimated by using an actual measurement and information gained from previous measurements. Usually, filtering is performed in real time.

2.2.3 Prediction

In figure 6 (c), the actual state of a process entity shall be estimated by using a history of previous measurements. The prediction problem requires an adequate system model in order to produce a meaningful estimation. Typically, the prediction is performed in real time. Figure 6 illustrates the different cases. Many filtering algorithms cover all three aspects. Filtering and prediction are fundamental elements of any tracking system. They are used to estimate present and future kinematic quantities such as position, velocity, and acceleration.

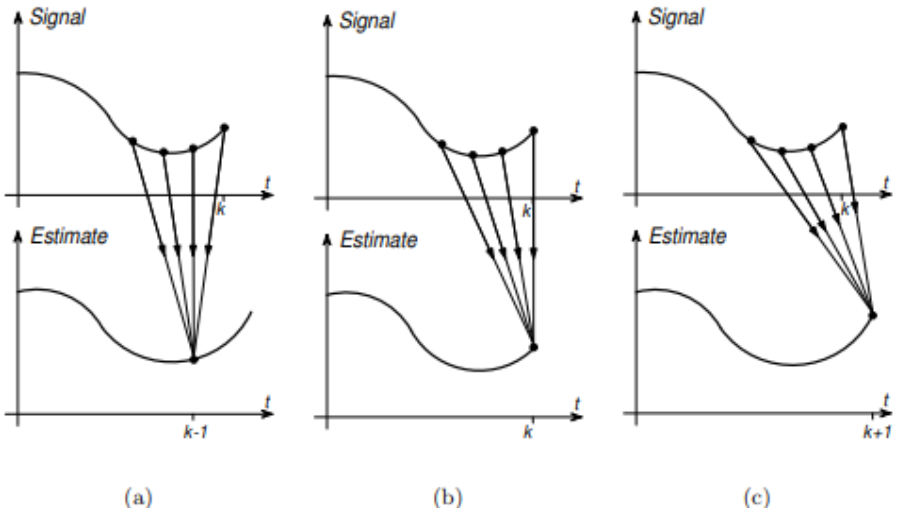

Figure 6. Smoothing (a), filtering (b), and prediction (c)

2.3 Sensor Fusion Example

Multi-sensor data fusion is important for achieving information complementarity, improving target tracking accuracy and recognition capabilities, and enhancing the system's anti-jamming.

The Figure 7 shows that the multi-sensor target fusion tracking can avoid the limitations of a single sensor, and improve the accuracy of target tracking. By combining data from the cameras, HMD and, LED's the maximum translational error was reduced, and the estimation of the head pose was accurately sensed, by taking into account the uncertainties are explicitly calculated.

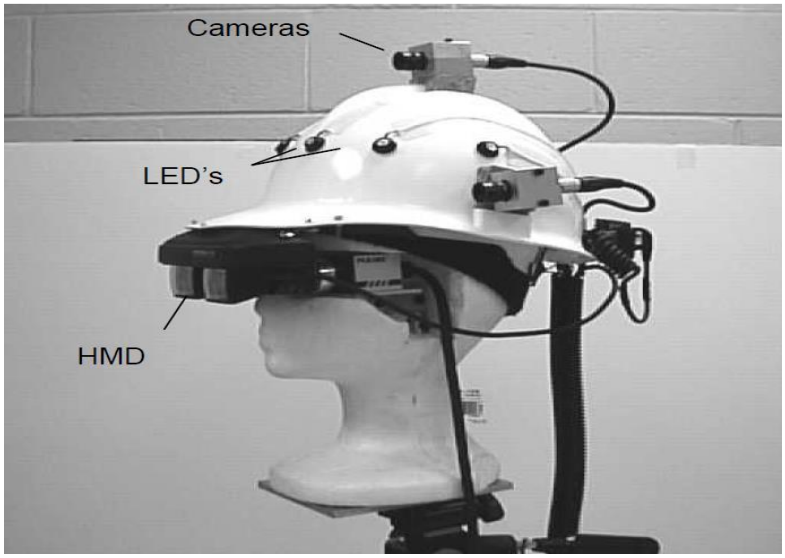

Figure 7. HMD and fixed sensors

Figure 8 illustrates users wearing an HMD being in the same spatially aligned model, having an independent control of their viewpoint and different layers of the data to be displayed. The setup serves computer supported cooperative work and enhances cooperation of visualization experts, due to the sensor fusion applied techniques. Each subject was focusing on a virtual object, that it was placed in the center of the VR world, while one subject manipulates the environment with a 3D mouse. And thanks to the magnetic tracker, both subjects can move accurately in a VR environment, this magnetic tracker enables the multi-tracking performance along with a real time application.

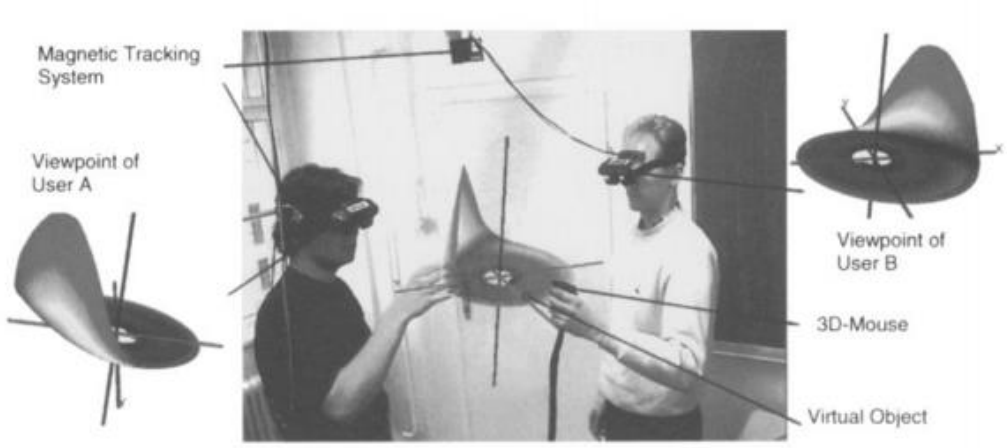

Figure 8. Tracking system

2.4 Theory of Kalman Filter

The Kalman Filter has many applications in mobile robotics ranging from perception to position estimation, and to control. This filter formulation is fairly general. This generality is possible because the problem has been addressed

- In 2D/3D
- In state space, with an augmented state vector
- Asynchronously
- With tensor calculus measurement models

The formulation has wide ranging uses. Some of the applications include:

- As the basis of an object position estimation system
- As the dead-reckoning element and overall integration
- As the mechanism for map matching in mapping applications
- As the identification element in adaptive control applications

In figure 9, Kalman filter can be represented as a control system in which has state diagram. The state of the system can be represented as a vector within that space. The internal state

variables are the smallest possible subset of system variables that can represent the entire state of the system at any given time. The minimum number of state variables required to represent a given system, n, is usually equal to the order of the system's defining differential equation. If the system is represented in transfer function form, the minimum number of state variables is equal to the order of the transfer function's denominator after it has been reduced to a proper fraction. It is important to understand that converting a state-space realization to a transfer function form may lose some internal information about the system, and may provide a description of a system which is stable, when the state-space realization is unstable at certain points.

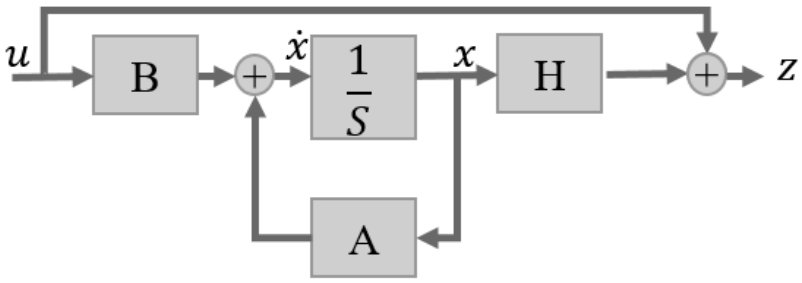

Figure 9. State diagram

Equation (6) and (7) are the mathematical representation of the Kalman filter state diagram in figure 9:

$$x_{k+1} = A_k x_k + B_k u_k \tag{6}$$

$$z_{k+1} = H_{k+1} x_{k+1} \tag{7}$$

where:

Variable	Meaning
x_k	State vector
z_k	Output vector
u_k	Input (or control) vector
A_k	State matrix
B_k	State vector
H_k	Output matrix

Table 1. Kalman filter formula variables.

In order to achieve an accurate final state, Kalman filter uses two processes: **prediction** and **correction.**

In figure 10, after the information is gathered, the process is able to start. As an iterative process, all the previous estimates will be the input for the current state. In order to have an accurate estimation, the most crucial Kalman filter variables are R and Q. For dynamic applications, R and Q are not rather simple to find out, because, in general, the noise is random along the time. Hence, finding out R and Q is not evident. There is not a proper method to find them but the tuning them. Kalman filter algorithm can be roughly organized under the following steps:

1. Making a prediction of a state, based on some previous values and system model.
2. Obtaining the measurement of that state, from the sensor.
3. Updating the prediction, based on the errors
4. Repeat.

Oculus Touch VR controller and an IMU 9 DOF motion are the sensors implemented in this study, Oculus touch gives information such previous state of the measurements, and IMU 9 DOF sensor provides acceleration data.

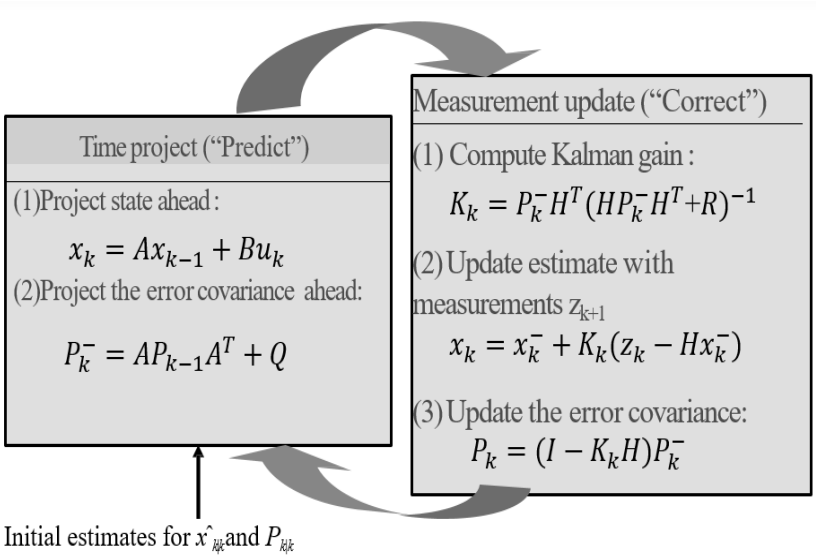

Figure 10. Kalman filter iteration process

where:

Variable	Meaning
K_k	Kalman gain
P_k	Measurement covariance
R	State covariance
H	Observable matrix ([0 1])
x_k	State vector

Table 2. Kalman filter iteration variables.

2.5 System Model for Kalman Filter

In figure 11, for the implementation of a Kalman filter algorithm, it is vital to know the system model of the application. In this study, the equation of motion represents the system model as is shown. Oculus Touch tracking controller and IMU are the sensors implemented in this study, Oculus touch will give information such previous state of the measurements, and IMU sensor provides acceleration data.

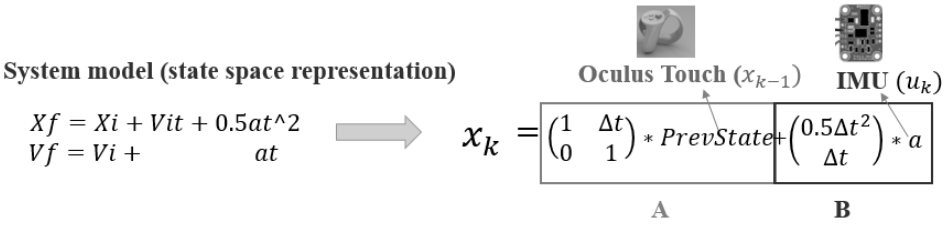

Figure 11. System mathematical model representation

3. Implementation of the VR System

3.1 System Architecture

Figure 12 shows the architecture of the whole system. The system is composed into two different parts, such as hardware and software. The subject wears the HMD and takes the forceps in order to perform the experiments. The forceps is connected to an electronic board which takes the acceleration and the rotational information from an IMU in a real-time task. Meanwhile, the VR controller is connected to the workstation and it is sending position data to Kalman filter algorithm that will merge the data from the acceleration data previously taken as well. Finally, the subjects can see their performance displayed in the HMD.

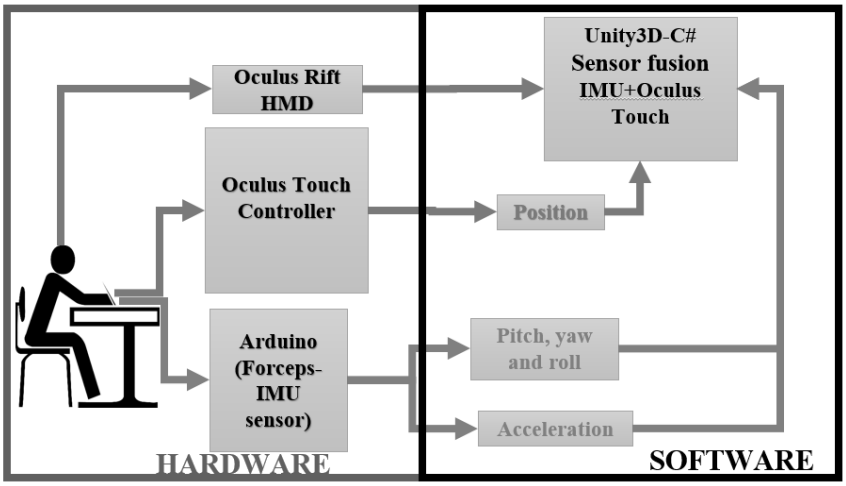

Figure 12. The architecture of the system

3.2 Hardware System

Figure 13 shows the hardware components of the system. It is composed by a VR controller that takes every 2-D position when is moved, a forceps and IMU sensor is attached to the controller in a one-piece structure. The Arduino reads the data from IMU and finally, the linear stage enables the free motion of the one-piece structure. In order to watch the virtual world, the subject has to wear the HMD, in which all the virtual environment is displayed.

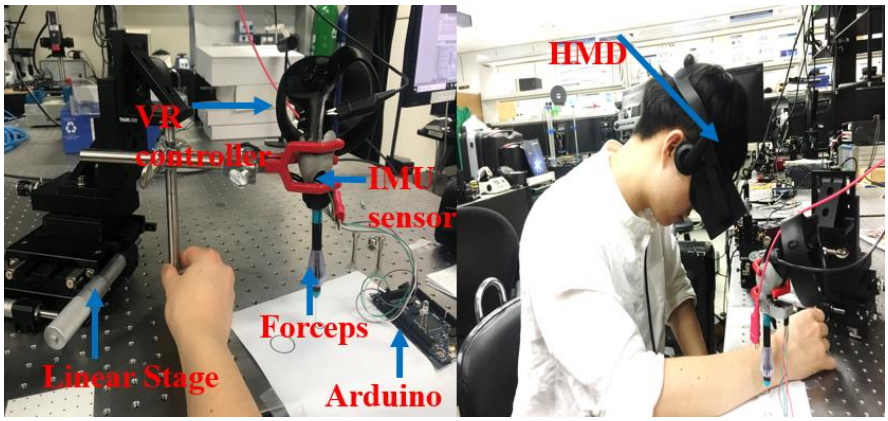

Figure 13. Hardware architecture

3.3 Software System

Figure 14 is showing the architecture of the software. The system was programmed in two different programming languages. In the electronic part, an IMU sensor is sending

acceleration data to Arduino system through an I2C communication protocol, which is based on C/C++. The Arduino is taking the IMU data and sending to Unity C# based software through an RS232 communication protocol. In Unity3D software, all the graphics and VR environment were implemented. Hence, the HMD graphics are coming directly from computational Unity software models.

Figure 14. Software architecture

3.4 General Schematic of the System

Figure 15 shows the schematic of the whole system. By having VR hardware elements such as HMD and VR controller, and an Arduino connected to the workstation, it makes possible a real-time simulation process. Besides, the external electronic part was an IMU sensor (9 DOF sensor), which sent information to Arduino. The VR controller, the IMU and the forceps were placed on a same one-piece structure.

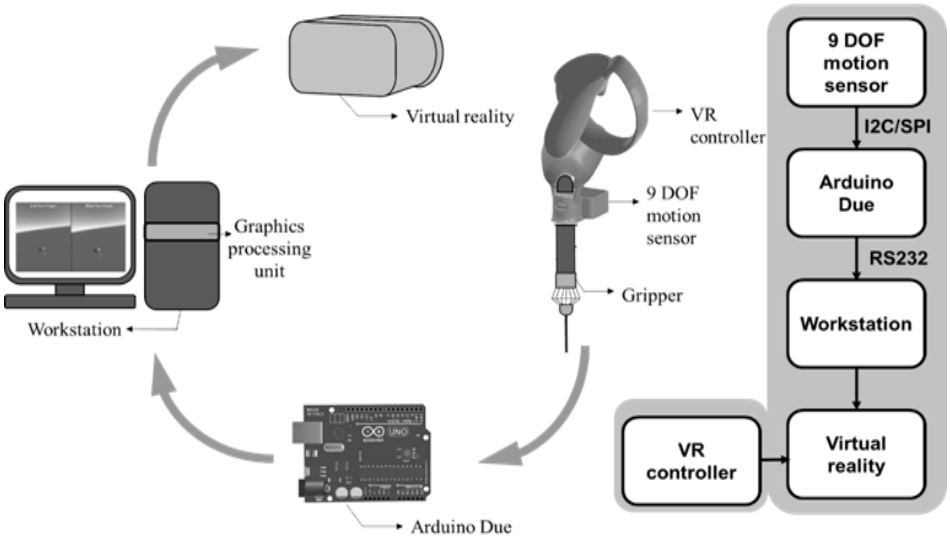

Figure 15. The general schematic of the system

4. Experiments

We designed a position matching task in which was divided into two different conditions:

- **Condition 1: Location tracking without Kalman filter**
    - High peak of deviations
- **Condition 2: Location tracking with Kalman filter activated**
    - High accuracy

To demonstrate Kalman filter performance in VR micro-environment, we applied human/non-human experiments with the previously mentioned conditions:

- Single axis dot by dot
- Motorized trace
- 2-D axis trace

4.1 Single Axis Dot by Dot

Figure 16 shows the distribution of the points along the VR space. Each dot has a separation of 1 mm. In the dot by dot experiment, we asked the subjects to stay in one position for 10 seconds in 3 different locations along the Y axis in the VR environmental space.

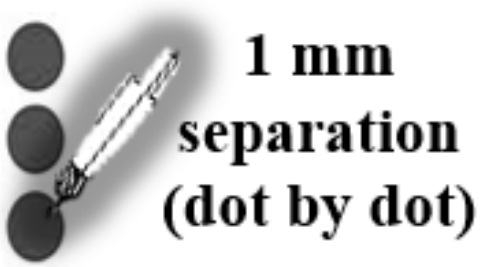

Figure 16. Dot by dot experimental environment

Figure 17 shows the action of the Kalman filter for a stationary dot by dot task, along with the Y-axis and starting in x=0 and y=0. It is noticeable a deviation in every point with No Kalman filter activated. The implementation of the Kalman filter makes the system to follow more accurately the reference. The results show that the algorithm proposed achieves efficient tracking of a stationary object under VR environments.

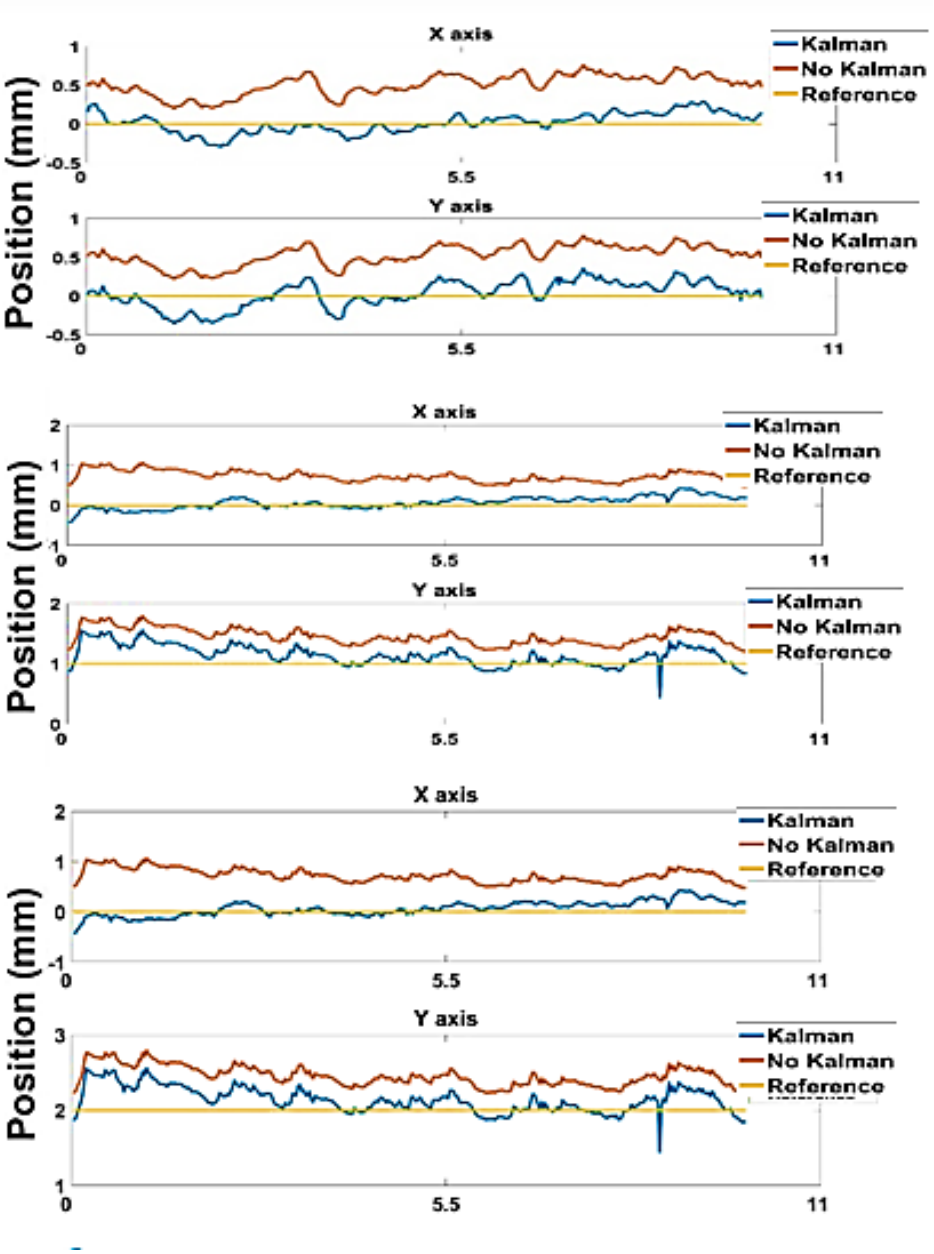

Figure 17. Dot by dot experimental result

Table 3 is showing that always when Kalman filter is activated, there is an accurate tendency to follow the reference comparing when Kalman filter is deactivated. In every axis, the improvement is noticed for more than 30% in most of the cases. The improvement might be more if we change the task into a dynamic case because the Kalman filter algorithm was implemented for dynamic models.

RMSE result (mm)						
	Condition 1		Condition 2		Improvement (%)	
Dot	X	Y	X	Y	X	Y
1	0.5224	0.542	0.1281	0.1705	39.43	37.15
2	0.5224	0.9859	0.1281	0.4931	39.43	49.28
3	0.5224	1.9786	0.1281	1.4807	39.43	49.79

Table 3. Dot by dot experimental RMSE result

4.2 Motorized Trace

4.2.1 X axis

Figure 18 is showing the forceps distance traveled by using a linear motor which moved it along the X-axis with a trapezoidal motion along 2 mm distance.

Figure 18. X-axis motorized trace

In figure 19, a trapezoidal move profile was used with the stage, in which the velocity was carried up to maximum velocity through a constant acceleration and then travel at that target velocity for a specified time or distance.

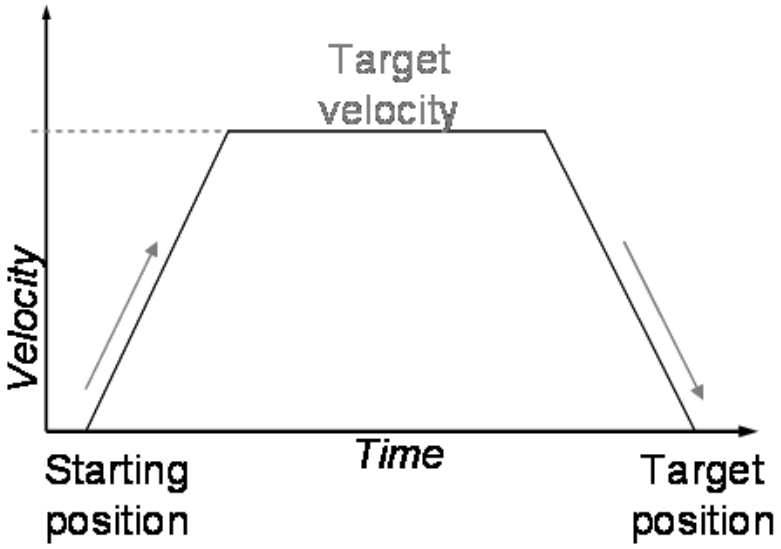

Figure 19. The motor trapezoidal motion

For this study, the target velocity was 0.25 mm/s.

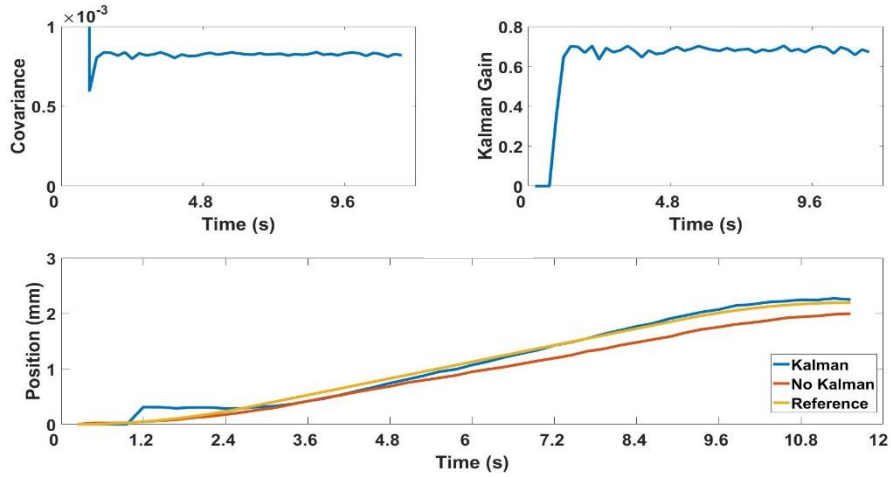

Figure 20. X-axis motorized trace result

As we know, there is noise in every system. In figure 20, the measurement covariance P is the noise in the process - if the system is a moving task, there will be slight variations in the speed due to bumps, hills, winds, and so on. P tells how much variance and covariance there is. Hence, figure 20 shows the updated covariance P along the time and also, the Kalman gain. It is notable the accuracy when the Kalman filter is activated, without Kalman filter, the deviation is high from the beginning of the task.

4.2.2 Y axis

Figure 21 is showing the forceps distance traveled by using a linear motor which moved it along the Y-axis with a trapezoidal motion along 2 mm distance.

Figure 21. Y-axis motorized trace

For this study, the target velocity was 0.25 mm/s.

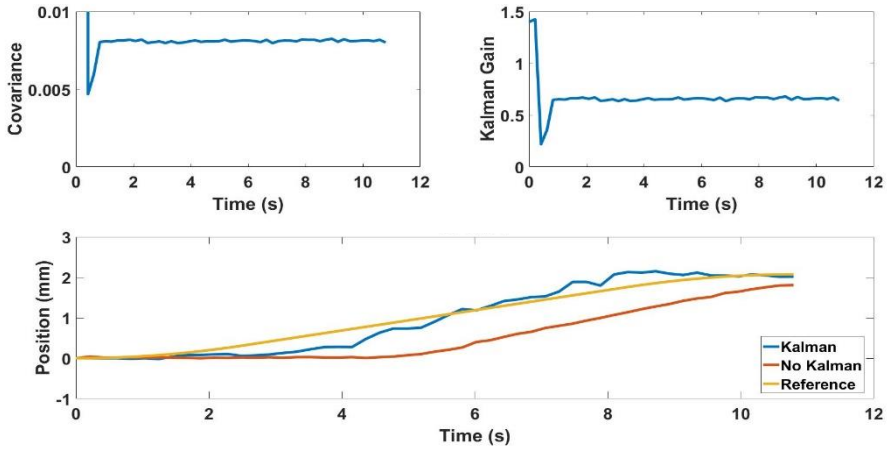

Figure 22. Y-axis motorized trace result

Figure 22 shows the updated covariance P along the time and the Kalman gain performance in the Y-axis as well. It is notable the accuracy when the Kalman filter is activated, without Kalman filter the deviation is high from the beginning of the task.

Notice that the filter quickly adapts to the reference value in both cases (X and Y axis). Note the Kalman gain acts as a regulator between our estimate and the measurement. The Kalman gain 'decides' based on an error from previous estimations, which of either the estimate or measurement to give more weight to. Intuitively, if we are making a good prediction, then the Kalman gain works to cancel out the effect of new measurements, but if we are making bad estimates, then it gives weight to the new measurements to make subsequent predictions.

4.3 *2-D* Axis Trace

We designed two different scenarios for this experiment. Figure 23 shows two scenarios:

a) **Printed circle**: A 10 mm diameter circle printed on a sheet of paper.

b) **VR circle**: A 10 mm diameter virtual circle.

We asked to 5 well-health subjects to follow the edge of the circle with the forceps in the printed circle and VR circle scenarios.

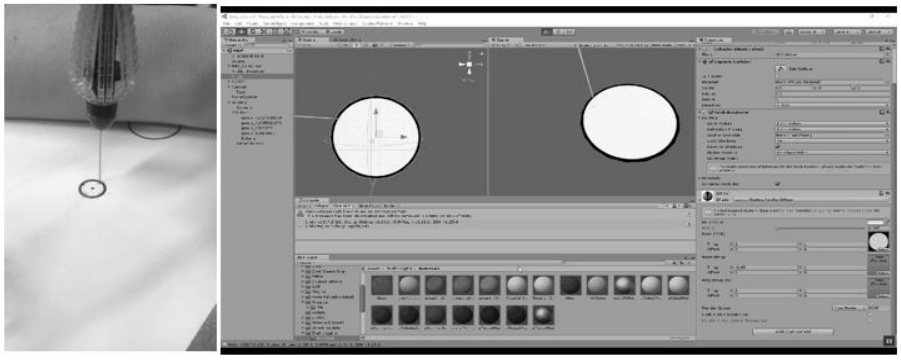

Figure 23. (a) Printed circle. (b) VR circle

4.3.1 2-D printed circle

Figure 24 shows the subject following the printed circle edge with eye-naked. By using a stage in order to move and fixed in one axis the forceps, each subject was asked to follow the edge of the printed circle without using an HMD. During this task, each subject performs one practice trial before starting with the experiment.

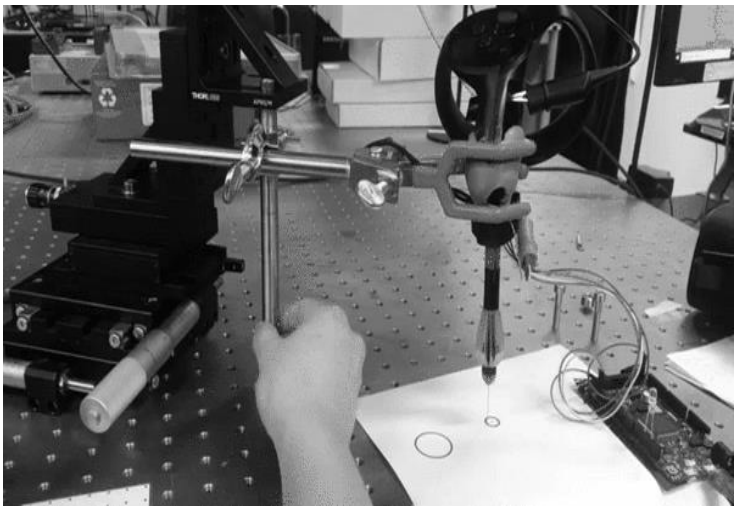

Figure 24. Subject performing the 2-D printed circle experiment

The results in figures 25 and 26 show the performance of each subject in a real-time task while performing the 2-D printed circle experiment with one hand. The Kalman filter activated algorithm has more precise data in order to follow the reference. The no Kalman result is always having a considerable deviation comparing with Kalman filter activated. The graphs show the 2D position of the trace with sensor fusion activated (Kalman) and sensor fusion deactivated (No Kalman) for each subject along the 10 mm circle (Reference). The subject's trace did not have any common starting point, each subject took their own time to start and finish the task. In addition, the condition 1 (No Kalman) and condition 2 (Kalman) were running at the same time the whole experiment with all participants.

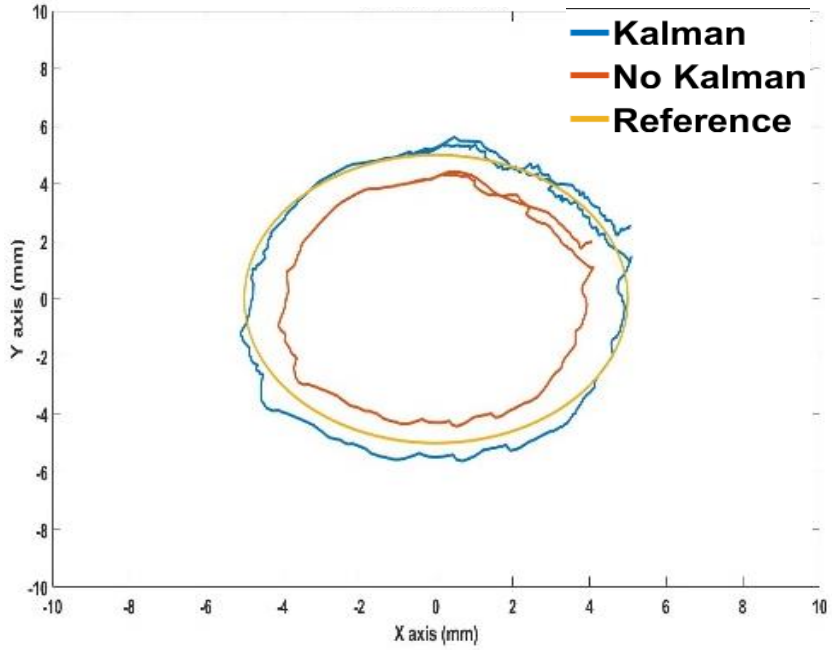

Figure 25. Subject 1-2D printed circle trace

In Table 4, the Root Mean Square Error (RMSE) from condition 1 (No Kalman) and condition 2 (Kalman) of a 2-D printed circle trace are compared. The condition 2 denotes more accuracy than condition 1, which in most of the cases the improvement was more than 55%.

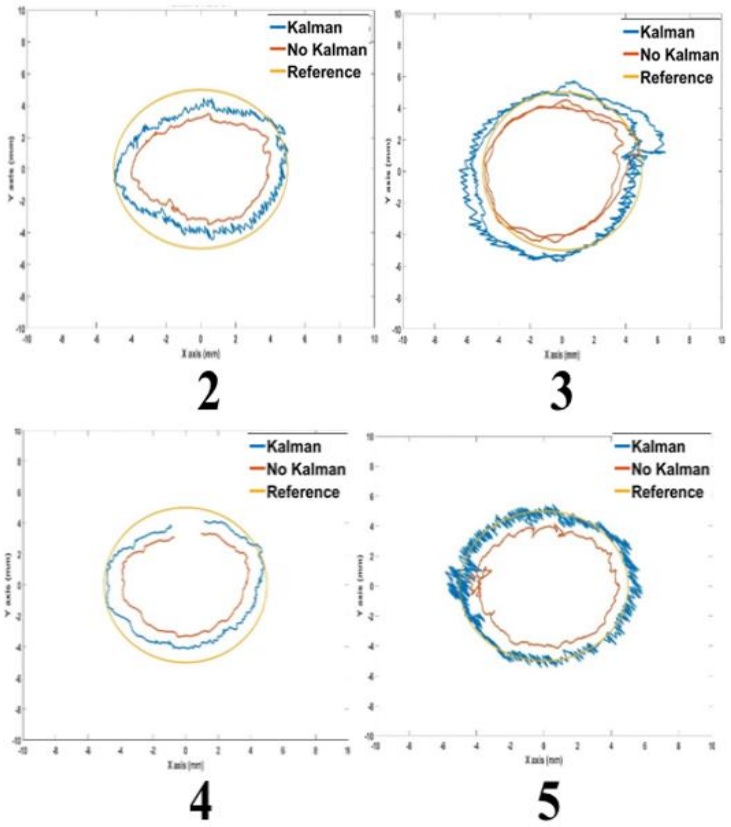

Figure 26. Subject 2 to 5-2D printed circle trace

Subject	RMSE Condition 1 (mm)	RMSE Condition 2 (mm)	Improvement (%)
1	0.8889	0.3306	55.83
2	1.5270	0.8169	71.01
3	0.7986	0.6677	13.09
4	1.4512	0.7022	74.90
5	0.9671	0.3458	62.13

Table 4. 2-D printed circle experimental RMSE result

4.3.2 VR circle

Each subject was asked to follow the edge of a VR 2D circle by wearing an HMD, by using a stage, the subject was able to move the forceps, which was fixed in one axis. Figure 27 shows the subject following the VR circle. The VR world can be explored interactively at a workstation, usually by manipulating keys or the mouse so that the content of the image moves in some direction or zooms in or out. Hence the interaction of the VR world was more intuited for the subject. The designed VR system encompasses the sense of presence, which is the point where the subject brain believes that is somewhere it is really not, and is accomplished through purely mental and/or physical means. The subjects experienced a state of total immersion that exists when enough senses are activated to create the perception of being present in a non-physical world.

- Mental immersion - A deep mental state of engagement, with the suspension of disbelief that one is in a virtual environment.
- Physical immersion - Exhibited physical engagement in a virtual environment, with the suspension of disbelief that one is in a virtual environment.

For virtual reality experiences, the element of interaction is crucial. It provides to users enough comfort for a naturally engaging time with the virtual environment. If the virtual environment responds to a user's action in a natural manner, excitement and senses of immersion will remain. If the virtual environment cannot have a fast response, the human brain will quickly notice and the sense of immersion will diminish. Virtual environment responses to interaction can include the way a participant moves around or changes in their viewpoint; generally through movements of their head. Hence, in this study, we used a real forceps.

Figure 27. VR circle tracing performed by a subject

The figures 28 and 29 show the 5 subjects performance in the VR environment while following the edge of a VR circle. Each subject was wearing an HMD which a 2D virtual circle was displayed, through the stereoscopic vision that the HMD has. Before the experiment was starting, each subject had the opportunity to practice in order to get along with the VR environment. The precision of the trace of each subject was more noticeable thanks to the visual stimuli that the HMD executes on the human eye, each subject followed the edge more accurately than in the printed circle scenario. The perspective that the VR world offered to the subject helped for a better performance compared with the 2D printed circle case.

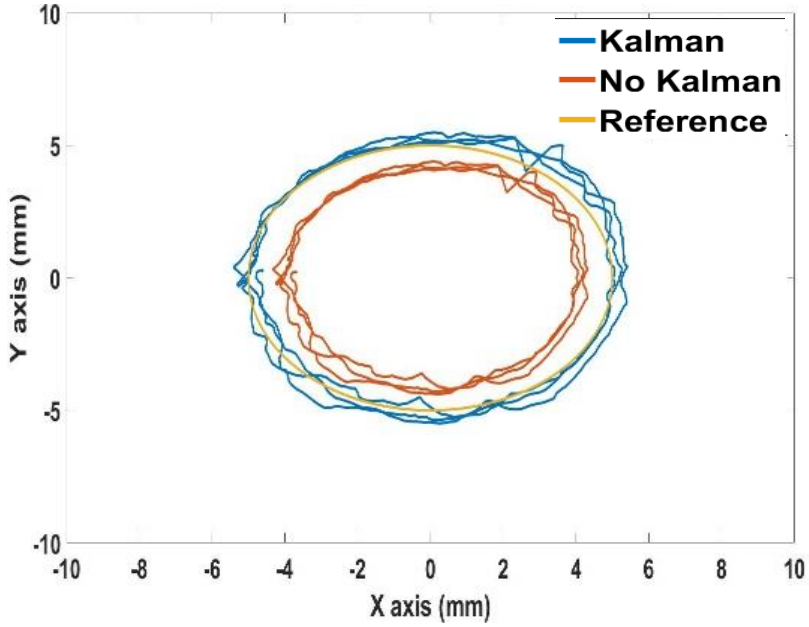

Figure 28. Subject 1-VR circle tracing result

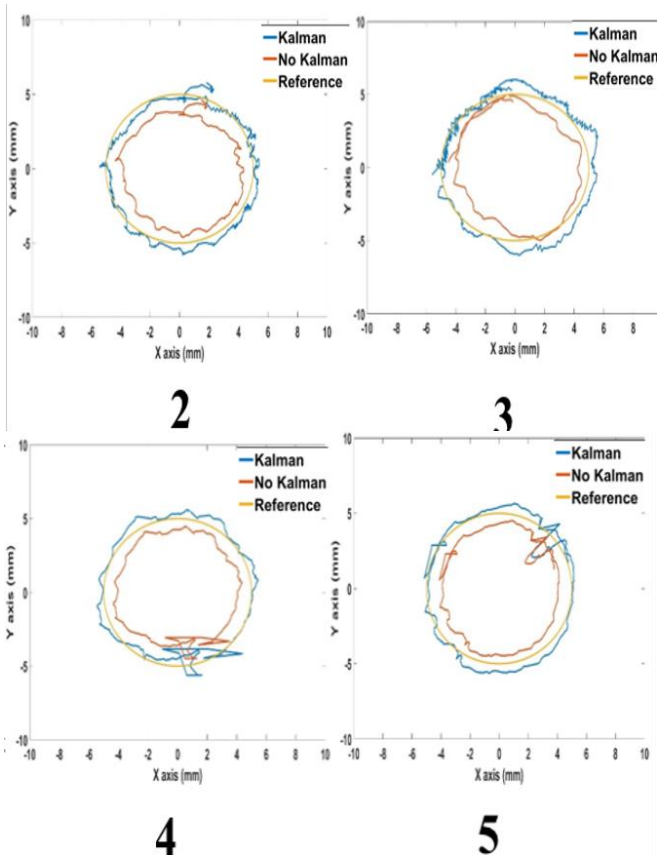

Figure 29. Subject 2 to 5-VR circle trace

Subject	RMSE Condition 1 (mm)	RMSE Condition 2 (mm)	Improvement (%)
1	0.8824	0.3172	56.52
2	0.9115	0.3852	52.63
3	0.7375	0.4755	26.62
4	0.9073	0.3924	51.49
5	0.8586	0.4206	62.13

Table 5. VR circle experimental RMSE result

In Table 5, the Root Mean Square Error (RMSE) from condition 1 (No Kalman) and condition 2 (Kalman) of a VR circle trace are compared. The VR in this study shows that the subject is able to have a greater control over stimulus presentation; variety in response options; presentation of stimuli in three or two dimensions. The condition 1 (No Kalman) and condition 2 (Kalman) were running at the same time the whole experiment with all participants. At the time when the experiment was running, the subjects were watching the VR environment under the condition 2 parameters. The impact of this VR technology was seen in the condition 2, which shows a patron that does not exceed 0.5 mm compared with the printed circle experiment. Besides in most of the cases, we found more than 50% improvement.

5. Discussion and Conclusion

The theory of a sensor fusion algorithm was validated in a C# real-time application, and by using VR technologies. In every single experiment, the response of the use of the fusion sensor algorithm showed improvements compared with the traditional tracking system, in most of the scenarios the improvement was more than 50%.

This VR technology enables the subject to have a precise and independent manipulation of the geometric and photometric relationships between objects; the possibility of examining sophisticated complex participants behaviors was noticed. Virtual reality and Kalman filter are the keys to control micro-locations in the VR space. The experiments conducted in this study showed a potential of decreasing of deviations when the Kalman filter is activated.

For future works, the Kalman filter will help the subjects to minimize hand tremor more clearly, and thus to have better control over their hand tremor. And with the help of the VR, different kind of scenarios can be made in order to train the future surgeons in any kind of field.

REFERENCES

1. R. Herbert, “Shaking when stirred: mechanisms of physiological tremor,” J. Physiol., vol. 590(Pt 11), pp.2549, May. 2012.

2. B. C. Becker, R. A. MacLachlan, L. A. Lobes Jr. and C. N. Riviere, “Semi automated intraocular laser surgery using handheld instruments,” Lasers Surg. Med., vol. 42, no. 3, pp. 264-273, Mar. 2010

3. C. Song, P. L. Gehlbach, and J. U. Kang, “Swept source optical coherence tomography based smart handheld vitreoretinal microsurgical tool for tremor suppression,” in Proc. 34th Annul. IEEE Engineering in Medicine and Biology Conference (EMBC), USA, Aug. 2012, pp. 1405-1408.

4. S. Konishi, M. Nokata, O. Jeong, S. Kusuda, T. Sakakibara, M. Kuwayama, and H. Tsutsumi, "Pneumatic micro hand and miniaturized parallel link robot for micro manipulation robot system," Proceedings 2006 IEEE International Conference on Robotics and Automation, 1036-1041, (2006).

5. B. Kaushal Kumar, L. Wei-kai, and C. Chun-yen, “A cost-effective interactive 3D virtual reality system applied to military live firing training,” Springer-Verlag, 127-140, (2016).

6. J.L. Maples-Keller, C. Yasinski, N. Manjin, “Virtual Reality-Enhanced Extinction of Phobias and Post-Traumatic Stress,” N. et al. Neurotherapeutics, 1–10, (2017).

7. B. Bideau, R. Kulpa, N. Vignais, S. Brault, F. Multon, and C. Craig, “Using Virtual Reality to Analyze Sports Performance,” in IEEE Computer Graphics and Applications 30(2),14-21, (2010).

8. J. W. V. de Faria, M. J. Teixeira, L. de Moura Sousa Júnior, J. P. Otoch, and E. G. Figueiredo, “Virtual and stereoscopic anatomy: when virtual reality meets medical education,” Journal of neurosurgery, 125(5), 1105-1111, (2016).

9. S. Faroque, B. Horan, and M. Joordens, “Keyboard control method for virtual reality micro-robotic cell injection training,” 10th System of Systems Engineering Conference (SoSE), 416-421, (2015).

10. J. Alex, B. Vikramaditya, and B.J. Nelson, “A virtual reality teleoperator interface for assembly of hybrid MEMS prototypes,” Proceedings of DETC ASME Design Engineering Technical Conference, pp. 5836, (1998).

11. Y. Vélaz, Arce J. Rodríguez, T. Gutiérrez, A. Lozano-Rodero, and A. Suescun, “The Influence of Interaction Technology on the Learning of Assembly Tasks Using Virtual Reality,” ASME. J. Comput. Inf. Sci. Eng. (12), 1121, (2014).

12. C. Batista, V. Seshadri, R. Augusto, P. Reinhardt, P. Moreira, and J. Batista, “Applying virtual reality model to green ironmaking industry and education: ‘a case study of

charcoal mini-blast furnace plant',” Transactions of the Institutions of Mining and Metallurgy C126(1-2), (2017).

13. B. Takacs, and L. Simon, “A clinical virtual reality rehabilitation System for phobia treatment,” 11th International Conference Information Visualization (IV'07), 798-806, (2007).

14. S. Sozzi, A. Monti, D. Nunzio, M. C. Do, and M. Schieppati, “Sensori-motor integration during stance: time adaptation of control mechanisms on adding or removing vision,” Hum. Mov. Sci. 30(2), 172–189, (2011).

15. G. Jin, and S. Nakayama, “Virtual reality game for safety education,” International Conference on Audio, Language and Image Processing, Shanghai, 95-100, (2014).

16. S. Benford, J. Bowers, L. E.Fahlén, and C. Greenhalgh, “Managing mutual awareness in collaborative virtual environments,” In Proceedings of the conference on Virtual reality software and technology, 223-236, (1994).

17. C. Carlsson, and O. Hagsand, “DIVE A multi-user virtual reality system,” In Virtual Reality Annual International Symposium, 394-400, (1993).

18. D. Reid, “The influence of virtual reality on playfulness in children with cerebral palsy: a pilot study,” Occupational Therapy International, 11(3), 131-144, (2004).

19. B. K. Wiederhold, and M. D. Wiederhold, “Three-year follow-up for virtual reality exposure for fear of flying,” Cyberpsychology and Behavior, 6(4), 441-445(2003).

20. J. McComas, and H. Sveistrup, “Virtual Reality Applications for Prevention, Disability Awareness, and Physical Therapy Rehabilitation in Neurology: Our Recent Work,” Journal of Neurologic Physical Therapy, 26(2), 55-61 (2002).

21. B. C. Becker, R. A. MacLachlan, L. A. Lobes, G. D. Hager, and C. N. Riviere, “Vision-based control of a handheld surgical micromanipulator with virtual fixtures,” IEEE Transactions on Robotics, 674-683, (2014).

22. T. Y. Fang, P. C. Wang, C. H. Liu, M. C. Su, and S. C. Yeh, “Evaluation of a haptics-based virtual reality temporal bone simulator for anatomy and surgery training,” Comput. Methods Programs Biomed 113(2), 674–681, (2014).

23. S. G. Kang, B. J. Ryu, K. S. Yang, Y. H. Ko, S. Cho, S. H. Kang, R. Patel, and J. Cheon, “An effective repetitive training schedule to achieve skill proficiency using a novel robotic virtual reality simulator,” J. of Surg. Edu 72(3), 369–376, (2015).

요 약 문

가상현실 미세수술환경에서의 정밀위치측정을 위한 센서융합

섬세한 미세 조작을 위해 피험자는 손 떨림을 효과적으로 최소화하면서 작업을 수행해야합니다. 최근에는 가상 현실 (VR) 미세 수술 시스템을 개발하여 교육 환경뿐 아니라 정확한 조작 작업을위한 시각적 피드백을 향상시킬 수있는 관심이 커지고 있습니다. 정확한 미세 위치 정보를 얻기 위해서는 정보 품질을 향상 시키거나 알고리즘에 대한 더 많은 정보를 얻기 위해 알고리즘을 통해 데이터를 결합하는 다양한 방법을 포함하는 다양한 센서 (센서 융합)의 사용이 필요합니다. 외과 용 도구 (예 : 포셉)의 정확한 위치 추적을 가능하게하기 위해 추가적인 관성 측정 장치 (IMU)를 갖춘 위치 추적 시스템을위한 센서 융합 알고리즘을 특징으로하는 VR 미세 수술 환경을 제안합니다. 시스템은 외과의가 시각적 인 피드백에서보다 정확한 감각을 갖도록 돕기 위해 외과 용기구 (즉, 포셉) 및 확대 된 두 눈금의 이미지를 재구성합니다. 우리는 두 개의 서로 다른 센서를 병합하고 칼만 필터 알고리즘으로 일치 시키면 마이크로 위치 파악이 더 정확할 것이라고 가정합니다. 우리는 (1) 칼만 필터가없는 위치 추적과 (2) 칼만 필터가 활성화 된 위치 추적의 두 가지 방법을 개발하고 테스트합니다. 오류에 대한 위치 추적의 성능 평가는 실제 및 가상 실험에서 수행되었습니다. 결과는 센서 융합이 활성화 된 상태가 칼만 필터 조건이없는 경우보다 더 정확한 위치 추적을 달성한다는 것을 보여줍니다.

키워드 : 가상 현실, 센서 융합, 칼만 필터, 미세 수술, 건강 관리.